

Supplementary Information (SI)

Hexachlorobenzene exerts genotoxic effects in a humpback whale cell line under stable exposure conditions

Jenny Maner^{§ 1,2}, Michael Burkard^{§ 1,3}, Juan Carlos Cassano⁴, Susan Bengtson Nash³, Kristin Schirmer*^{1,2,5}, and Marc J.-F. Suter^{1,2}

¹Eawag, Swiss Federal Institute of Aquatic Science and Technology, Department Environmental Toxicology, 8600 Dübendorf, Switzerland

²ETH Zürich, Department of Environmental Systems Science, 8092 Zürich, Switzerland

³Griffith University, Environmental Futures Research Institute, Southern Ocean Persistent Organic Pollutants Program, Brisbane, QLD 4108, Australia

⁴Empa, Swiss Laboratories for Material Science and Technology, Particle-Biology Interactions Laboratory, 9014 St Gallen, Switzerland

⁵EPF Lausanne, School of Architecture, Civil and Environmental Engineering, 1015 Lausanne, Switzerland

[§]These authors contributed equally

*Corresponding author

18 **Table of contents**

19 **1. Establishment of the passive dosing setup for HCB**

20	a.	Table S1: Equations characterising the partitioning between different phases in the	
21		passive dosing setup	p. S3
22	b.	Figure S1: Mass of silicone O-rings	p. S4
23	c.	Comparison of loading techniques	p. S5
24	d.	Table S2: Comparison of loading efficiencies (mean \pm SD) of partitioning loading and	
25		push loading	p. S6
26	e.	Estimation of HCB concentration in blood plasma of humpback whales	p. S7
27	f.	Figure S2: Time to steady-state and concentration stability during loading	p. S9
28	g.	Figure S3: Pre-equilibration of serum-free DMEM/F12 exposure medium	p. S9
29	h.	Figure S4: Stability of HCB concentration in a 24 well-plate in presence of cells	p. S10
30	i.	Table S3: Partitioning coefficients for HCB between LB, silicone (mass), and exposure	
31		medium DMEM/F12	p. S11
32	j.	Comparison of partitioning coefficients with published literature	p. S12
33	k.	Table S4: Comparison of published partitioning coefficients for HCB between reservoir	
34		and water	p. S12
35	l.	Table S5: Comparison of partitioning properties of HCB with 1,2-dichlorobenzene (1,2-	
36		DCB), 1,2,4-trichlorobenzene (1,2,4-TCB), and benzo[a]pyrene (B[a]P)	p. S13
37	m.	Figure S5: Re-use of O-rings	p. S14

38

39 **2. Effect of HCB on viability of HuWa_{TERT} cells**

40	a.	Figure S6: Impact of HCB exposure on viability of cells in monolayer under temperature	
41		stress	p. S15
42	b.	Figure S7: Impact of HCB exposure on viability of cells in monolayer with serum-free	
43		exposure medium	p. S16

44

45 **3. Genotoxic effects of HCB in HuWa_{TERT} cells**

46	a.	Figure S8: Visualisation of data obtained in four replicates of the comet assay	p. S17
----	----	---	---------------

47

48	4. References		p. S18
----	----------------------	--	---------------

49

50 **1. Establishment of the passive dosing setup for HCB**

51 **1.a. Table S1**

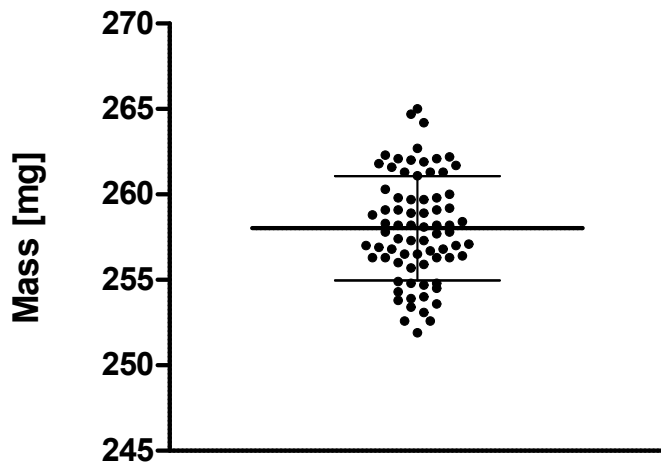
52 **Table S1. Equations characterising the partitioning between different phases in the passive dosing setup**

Efficiency of silicone O-ring loading	$Efficiency = \frac{m_{HCB,sil}^*}{m_{HCB,LB,t0}}$
Mass balance of silicone O-ring loading	$Recovery = \frac{m_{HCB,LB}^* + m_{HCB,sil}^*}{m_{HCB,LB,t0}}$
Partitioning coefficient between LB and silicone O-ring, based on the volume of silicone	$K_{LB:sil} = \frac{C_{LB}^*}{C_{sil}^*} = \frac{m_{HCB,LB}^*/V_{LB}}{m_{HCB,sil}^*/V_{sil}} \left[\frac{L}{L} \right]$
Predicted equilibrium concentration on silicone O-ring as a function of starting concentration in LB	$C_{sil}^* = \frac{C_{LB,t0}}{K_{LB:sil} + \frac{V_{sil}}{V_{LB}}}$
Starting concentration in LB required to achieve a specified equilibrium concentration on silicone O-ring	$C_{LB,t0} = C_{sil}^* \frac{V_{sil}}{V_{LB}} + C_{sil}^* K_{LB:sil}$
Partitioning coefficient between silicone O-ring and cell culture medium DMEM/F12, based on the volume of silicone	$K_{sil:DMEM/F12} = \frac{C_{sil}^*}{C_{DMEM/F12}^*} = \frac{m_{HCB,sil}^*/V_{sil}}{C_{DMEM/F12}^*} \left[\frac{L}{L} \right]$
Predicted equilibrium concentration in cell culture medium DMEM/F12 as a function of concentration on silicone O-ring	$C_{DMEM/F12}^* = \frac{C_{sil}^*}{K_{sil:DMEM/F12}}$
Theoretical partitioning coefficient between LB and in cell culture medium DMEM/F12	$K_{LB:DMEM/F12} = K_{LB:sil} \cdot K_{sil:DMEM/F12}$
Partitioning coefficient between LB and silicone O-ring, based on the mass of silicone	$K'_{LB:sil} = \frac{C_{LB}^*}{C_{sil}^*} = \frac{m_{HCB,LB}^*/V_{LB}}{m_{HCB,sil}^*/m_{sil}} \left[\frac{kg}{L} \right]$
Partitioning coefficient between silicone O-ring and cell culture medium DMEM/F12, based on the mass of silicone	$K'_{sil:DMEM/F12} = \frac{C_{sil}^*}{C_{DMEM/F12}^*} = \frac{m_{HCB,sil}^*/m_{sil}}{C_{DMEM/F12}^*} \left[\frac{L}{kg} \right]$

53 $m_{HCB,sil}^*$ - mass of HCB on silicone O-rings at equilibrium; $m_{HCB,LB,t0}$ - mass of HCB in loading buffer (LB) at the
54 beginning; $m_{HCB,LB}^*$ - mass of HCB in the LB at equilibrium; $K_{LB:sil}$ - partitioning coefficient between LB and silicone;

55 C_{LB}^* - equilibrium concentration in the LB; C_{sil}^* - equilibrium concentration in silicone; V_{LB} - volume of LB; V_{sil} - volume
56 of silicone; $C_{LB,10}$ - starting concentration in LB; $K_{sil:DMEM/F12}$ - partitioning coefficient between silicone and DMEM/F12;
57 C_{sil} - concentration in silicone[‡]; $m_{HCB,sil}$ - mass of HCB in silicone[‡]; $C_{DMEM/F12}^*$ - equilibrium concentration of HCB in
58 DMEM/F12. [‡]Due to the low solubility of HCB in aqueous solution the loss of HCB to the medium can be considered
59 negligible in comparison to the amount loaded onto the O-ring, thus C_{sil} and m_{sil} can be considered as constant and are
60 therefore not denoted as equilibrium concentrations¹.

61 1.b. Figure S1



62

63 **Figure S1. Mass of silicone O-rings.** O-rings from Hutchinson Suisse (Langnau am Albis, Switzerland). Error bars
64 represent mean with standard deviation (SD) (n = 75). Size of O-rings is highly standardised with a relative SD of only
65 1.2%.

66

67 **1.c. Comparison of loading techniques**

68 Two different methods of loading were compared: partitioning loading and push loading.
69 Partitioning loading is the most common approach in passive dosing assays. The working principle
70 of this technique is equilibrium partitioning of the chemical from a loading buffer (LB) — usually
71 methanol²⁻⁴ or a mixture of methanol and water¹ — to silicone. Hydrophobic chemicals
72 preferentially partition from the solution into the silicone. Partitioning loading was carried out as
73 described in section 2.2 of the main manuscript.

74 In push loading, a chemical is dissolved in methanol, followed by a stepwise addition of water,
75 thus decreasing the chemical's solubility in the LB and 'pushing' it into the silicone. Birch et al.
76 (2010) reported complete mass transfer of fluoranthene to silicone using this technique⁵. Push
77 loading was carried out as described in Birch et al. (2010)⁵ with modified volumes of LB. Briefly,
78 pre-cleaned O-rings were placed in 100 μL per O-ring of a solution of HCB in methanol. Then,
79 increasing volumes of dH_2O were added in 10 minute intervals as follows: 100 μL , 100 μL , 100
80 μL , 200 μL , 400 μL , 600 μL , to a final volume of 1.6 mL. O-rings were equilibrated in the LB for
81 24 hours with constant shaking at 250 rpm, then 10 mL of dH_2O were added, and O-rings were
82 equilibrated for another 24 hours. This technique was used with the following concentrations of
83 HCB in methanol: 100, 50, 10, and 0 (control) $\mu\text{g}/\text{mL}$.

84 To compare the two techniques the loading efficiency was determined (Table S2). Both push and
85 partitioning loading were efficient for loading considerable amounts of HCB onto O-rings.
86 However, partitioning loading was slightly more efficient, while at the same time more convenient
87 in terms of handling. The solubility of HCB in the LB of push loading would be predicted to be
88 lower than with partitioning loading where methanol content is 60% compared to 0.9% in push

89 loading after the addition of water. It can be reasoned that the rapidly decreasing amount of
90 methanol during push loading, instead of leading to partitioning into the silicone, might cause HCB
91 losses through evaporation or crystallisation. As a consequence, partitioning loading was chosen
92 for our passive dosing setup. A full mass balance calculation determined a recovery of $104 \pm 9\%$
93 ($n = 6$) for this technique, indicating no major losses in the process.

94

95 1.d. Table S2

96 **Table S2. Comparison of loading efficiencies (mean \pm SD) of partitioning loading and push loading**

	Partitioning loading	Push loading
Loading efficiency	84% \pm 10% (n=6)	74% \pm 10% (n=9)

97

98

99 **1.e. Estimation of HCB concentration in blood plasma of humpback whales**

100 i. Estimation based on partitioning coefficients for HCB between blubber and plasma developed
101 for bottlenose dolphins⁶

102 a) Based on wet-weight partitioning coefficient:

103 $C_{\text{blubber}} = 60 \rightarrow 200 \text{ ng/g}_{\text{lipid}(\text{blubber})}$ ⁷

104 $\text{Lipid}_{\text{blubber}} = \sim 50\%$ ⁷

105 $C_{\text{blubber}} = 60 \rightarrow 200 \text{ ng/g}_{\text{lipid}} \cdot 0.5 \text{ g}_{\text{lipid}}/\text{g}_{\text{blubber}} = 30 \rightarrow 100 \text{ ng/g}_{\text{blubber}}$

106 $K_{\text{blubber:plasma}} = 155$ (juveniles) / 94 (adult males) / 144 (adult females) (values for bottlenose
107 dolphins)⁶; partitioning coefficient for adult males was selected to avoid confounding factors
108 such as contaminant offload to offspring during reproduction

109 $C_{\text{plasma}} = 30 \rightarrow 100 \text{ ng/g}_{\text{blubber}} / 94 = 0.32 \rightarrow 1.06 \text{ ng/g}_{\text{plasma}} = \sim 0.32 \rightarrow \underline{1.06 \text{ ng/mL}_{\text{plasma}}}$

110 b) Based on lipid-normalised partitioning coefficient:

111 $C_{\text{blubber}} = 60 \rightarrow 200 \text{ ng/g}_{\text{lipid}(\text{blubber})}$ ⁷

112 $K_{\text{blubber:plasma}} = 1.54$ (juveniles) / 1.55 (adult males) / 1.17 (adult females) (values for bottlenose
113 dolphins)⁶; partitioning coefficient for adult males was selected to avoid confounding factors
114 such as contaminant offload to offspring during reproduction

115 $C_{\text{plasma}} = 60 \rightarrow 200 \text{ ng/g}_{\text{lipid}(\text{blubber})} / 1.55 = 38.7 \rightarrow 129.0 \text{ ng/g}_{\text{lipid}(\text{plasma})}$

116 $\text{Lipid}_{\text{plasma}} = \sim 0.5\%$ (values from bottlenose dolphins)⁶

117 $C_{\text{plasma}} = 38.7 \rightarrow 129.0 \text{ ng/g}_{\text{lipid}(\text{plasma})} \cdot 0.005 \text{ g}_{\text{lipid}}/\text{g}_{\text{plasma}} = 0.19 \rightarrow 0.65 \text{ ng/g}_{\text{plasma}} = \sim 0.19 \rightarrow$
118 $0.65 \text{ ng/mL}_{\text{plasma}}$

119

120 ii. Estimation based on physiologically based pharmacokinetic model of HCB distribution in a
121 humpback whale⁸

122 a) At the beginning of migration

123 $C_{\text{blubber}} = \sim 60 \text{ ng/g}_{\text{lipid}}$ ⁷

124 $C_{\text{blubber}} \sim 10\% \text{ higher than } C_{\text{plasma}}$ ⁸

125 $C_{\text{blubber}} = \sim 60 \text{ ng/g}_{\text{lipid}} \rightarrow C_{\text{plasma}} = \sim 54 \text{ ng/g}_{\text{lipid}}$

126 $\text{Lipid}_{\text{plasma}} = \sim 0.5\%$ (values from bottlenose dolphins)⁶

127 $\underline{C_{\text{plasma}}} = \sim 54 \text{ ng/g}_{\text{lipid}} \cdot 0.005 \text{ g}_{\text{lipid}}/\text{g}_{\text{plasma}} = 0.27 \text{ ng/g}_{\text{plasma}} = \underline{\sim 0.27 \text{ ng/mL}_{\text{plasma}}}$

128 b) At the end of migration

129 $C_{\text{blubber}} = \sim 200 \text{ ng/g}_{\text{lipid}}$ ⁷

130 $C_{\text{blubber}} \sim 35\% \text{ lower than } C_{\text{plasma}}$ ⁸

131 $C_{\text{blubber}} = \sim 200 \text{ ng/g}_{\text{lipid}} \rightarrow C_{\text{plasma}} = \sim 270 \text{ ng/g}_{\text{lipid}}$

132 $\text{Lipid}_{\text{plasma}} = \sim 0.5\%$ (values from bottlenose dolphins)⁶

133 $\underline{C_{\text{plasma}}} = \sim 270 \text{ ng/g}_{\text{lipid}} \cdot 0.005 \text{ g}_{\text{lipid}}/\text{g}_{\text{plasma}} = 1.35 \text{ ng/g}_{\text{plasma}} = \underline{\sim 1.35 \text{ ng/mL}_{\text{plasma}}}$

134

135 iii. Average

136 a) At the beginning of migration

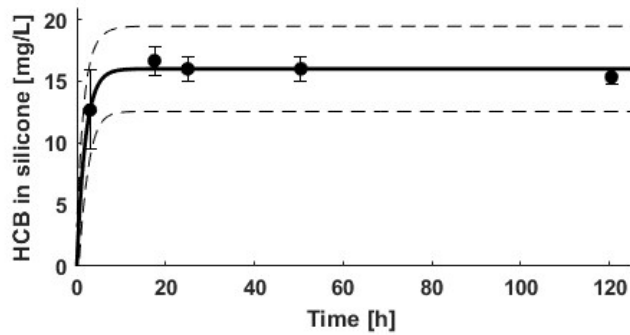
137 $\underline{C_{\text{plasma}}} = \sim (0.32+0.19+0.27)/3 = \underline{0.3 \text{ ng/mL}_{\text{plasma}}}$

138 b) At the end of migration

139 $\underline{C_{\text{plasma}}} = \sim (1.06+0.65+1.35)/3 = \underline{1 \text{ ng/mL}_{\text{plasma}}}$

140

141 1.f. Figure S2

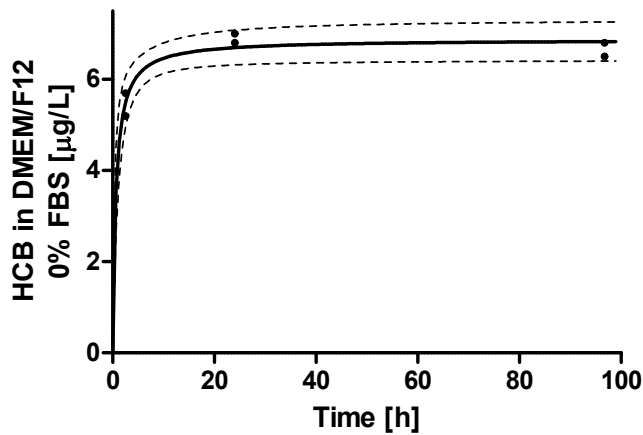


142

143 **Figure S2. Time to steady-state and concentration stability during loading.** Loading of silicone O-rings by
144 partitioning from a loading buffer of methanol/water 60:40 (v/v) at room temperature and 250 rpm. Each point represents
145 the mean of three technical replicates (i.e. three O-rings), error bars represent SD. Equilibrium was reached within 6 h
146 (see Fig. 1a), and remained stable for at least 120 h.

147

148 1.g. Figure S3



149

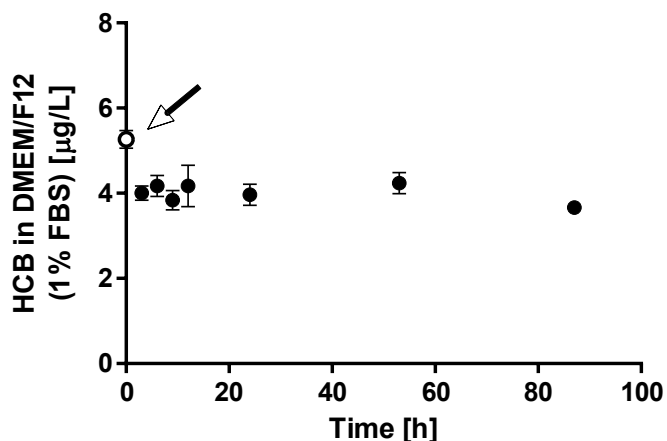
150 **Figure S3. Pre-equilibration of serum-free DMEM/F12 exposure medium.** Time to steady-state in DMEM/F12 (0%
151 FBS) with submerged HCB-loaded silicone O-rings in amber glass vials at 37°C and 250 rpm. Each point represents
152 one technical replicate.

153

154

155 **1.h. Figure S4**

156 Plastic foil, with which microtiter plates are commonly covered, has a high capacity for sorption
157 of hydrophobic chemicals, leading to lower exposure concentrations. In 24 well plates covered
158 with plastic foil (Figure S3) equilibrium was established at 20% lower medium concentrations as
159 compared to aluminium foil (see Figure 1c of the main manuscript).



160

161 **Figure S4. Stability of HCB concentration in a 24 well-plate in the presence of cells.** Concentration of HCB in
162 exposure medium DMEM/F12 (1% FBS) immediately after pre-equilibration (at 0 hours, open symbol \circ indicated by
163 arrow), and after transfer to a 24-well plate containing a confluent monolayer of cells (1×10^4 cells/cm² seeded two days
164 prior to exposure), with a loaded O-ring placed afloat and the plate covered with plastic foil, sealed with parafilm and
165 incubated at 37°C and 30 rpm (solid symbols \bullet). Each point represents the mean of three technical replicates, error
166 bars represent SD. After transfer of pre-equilibrated medium to the cell-containing 24-well plate there was a drop in
167 aqueous HCB concentration; equilibrium re-established at a lower concentration equal to 75% of the pre-equilibrated
168 concentration. This concentration remained stable for at least 87 hours.

169

170 **1.i. Table S3**

171 The partitioning coefficients for HCB between the three phases LB, silicone O-ring, and exposure
172 medium DMEM/F12 (with 1% FBS or without) can be determined in terms of volume (K) or mass
173 (K') of silicone. For the purpose of comparison with literature values both have been determined.
174 Partitioning coefficients K are given in Figure 1c (main manuscript), partitioning coefficients K'
175 are given in Table S3.

176

177 **Table S3. Partitioning coefficients for HCB between LB, silicone, and exposure medium DMEM/F12**

$\log K'_{\text{LB:sil}}$	$\log K'_{\text{sil:DMEM/F12}}$ (1%FBS)	$\log K'_{\text{sil:DMEM/F12}}$
-2.10	3.57	4.17

178

179

180 1.j. Comparison of partitioning coefficients with published literature

181 The HCB partitioning coefficients found here are in good agreement with previously published
182 partitioning coefficients for HCB (Table S4) and for other chlorobenzenes and benzo[a]pyrene
183 (B[a]P) (Table S5). There is a negative linear relationship between $\log K_{ow}$ and partitioning into
184 serum-free medium. The addition of serum increases partitioning to the medium of substances with
185 high $\log K_{ow}$ values, but has little influence on substances with low $\log K_{ow}$ values. HCB is more
186 hydrophobic than 1,2-dichlorobenzene (1,2-DCB) and 1,2,4-trichlorobenzene (1,2,4-TCB), but
187 less so than B[a]P. Consequently, it partitions less readily from silicone into medium, especially
188 serum-free medium, than the two chlorobenzenes, but more so than B[a]P.

189

190 1.k. Table S4

191 **Table S4. Comparison of published partitioning coefficients for HCB between reservoir and water**

Description	Partitioning Coefficient	Source
Partitioning coefficient for HCB between silicone and water	$\log K'_{sil:w} = 5.05$ [L/kg]	Gilbert et al. (2015) ⁹
Partitioning coefficient for HCB between octadecyl discs and water	$\log K_{disc:w} \approx 6.3$ [L/L]	Mayer et al. (1999) ¹⁰
Linear relationship of partitioning coefficients for PAHs from silicone to water based on their hydrophobicity: $\log K_{sil:w} = 0.799 \cdot \log Kow + 0.234$; applied to HCB	$\log K_{sil:w} = 4.81$ [L/L]	Smith et al. (2010) ⁴
Partitioning coefficient for HCB between silicone and DMEM/F12 (without FBS)	$\log K_{sil:DMEM/F12} = 4.25$ [L/L] $\log K'_{sil:DMEM/F12} = 4.17$ [L/kg]	This study

192

193

194 **1.1. Table S5**195 **Table S5. Comparison of partitioning properties of HCB with 1,2-dichlorobenzene (1,2-DCB), 1,2,4-**
196 **trichlorobenzene (1,2,4-TCB), and benzo[a]pyrene (B[a]P)**

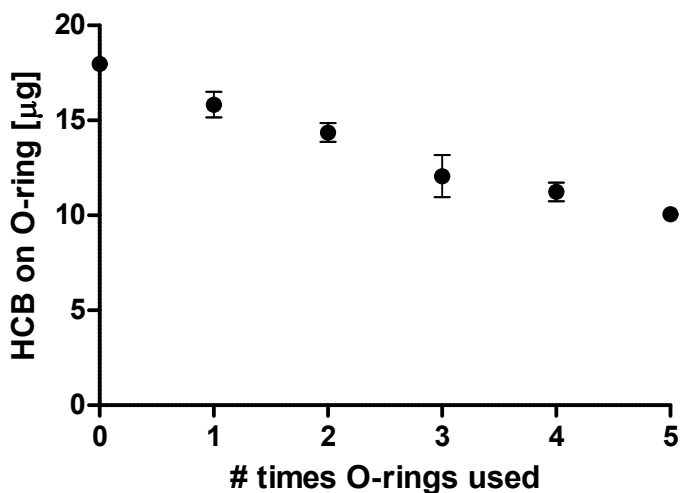
	$\log K_{ow}$	Henry's law constant [Pa·m ³ /mol]	$K_{LB:sil}^c$	$\log K_{sil:medium}^{(-)serum}^d$	$\log K_{sil:medium}^{(+serum)}^e$
HCB ^a	5.73	35 ^f	$6.56 \cdot 10^{-3}$	4.25	3.66
1,2-Dichlorobenzene ^b	3.43	195	$8.05 \cdot 10^{-2}$	3.53	3.54
1,2,4-Trichlorobenzene ^b	4.05	101	$3.8 \cdot 10^{-2}$	3.96	3.83
Benzo[a]pyrene ^b	6.13	0.034	$1.17 \cdot 10^{-2}$	5.08	2.39

197 ^aThis study; ^bData from Kramer et al. (2010)¹; ^cLB = MeOH/H₂O 60:40% (v/v); ^dData for HCB in DMEM/F12 medium,
198 data for 1,2-DCB, 1,2,4-TCB and B[a]P in L15 medium; ^eData for HCB in DMEM/F12 medium with 1% FBS, data for
199 1,2-DCB, 1,2,4-TCB and B[a]P in L15 medium with 5% FBS; ^fData from Jantunen and Bidleman (2006)¹¹

200

201 **1.m. Figure S5**

202 Relative to the medium concentration aimed for, quite large quantities of highly concentrated HCB
203 stock solutions are required to load O-rings. Thus, an experiment was carried out to assess the
204 possibility of re-using loaded O-rings. To this end, nine O-rings were loaded to the same
205 concentration and then used between 0 and 5 times to pre-equilibrate DMEM/F12 medium with
206 1% FBS for 24 hours, followed by 24 hours exposure in 24-well plates covered with aluminium
207 foil, sealed and incubated at 37°C and 30 rpm. After exposure the O-rings were extracted with
208 cyclohexane to analyse remaining HCB in silicone. After each cycle of pre-equilibration and
209 exposure there was a slight reduction in the concentration of HCB in silicone. Thus, used O-rings
210 cannot be used to achieve the same concentration. Yet, if the lower concentrations are taken into
211 account re-use is possible. Nevertheless, with the aim of our study being to perform exposures at
212 the same starting concentrations, we used freshly prepared O-rings in our experiments.



213

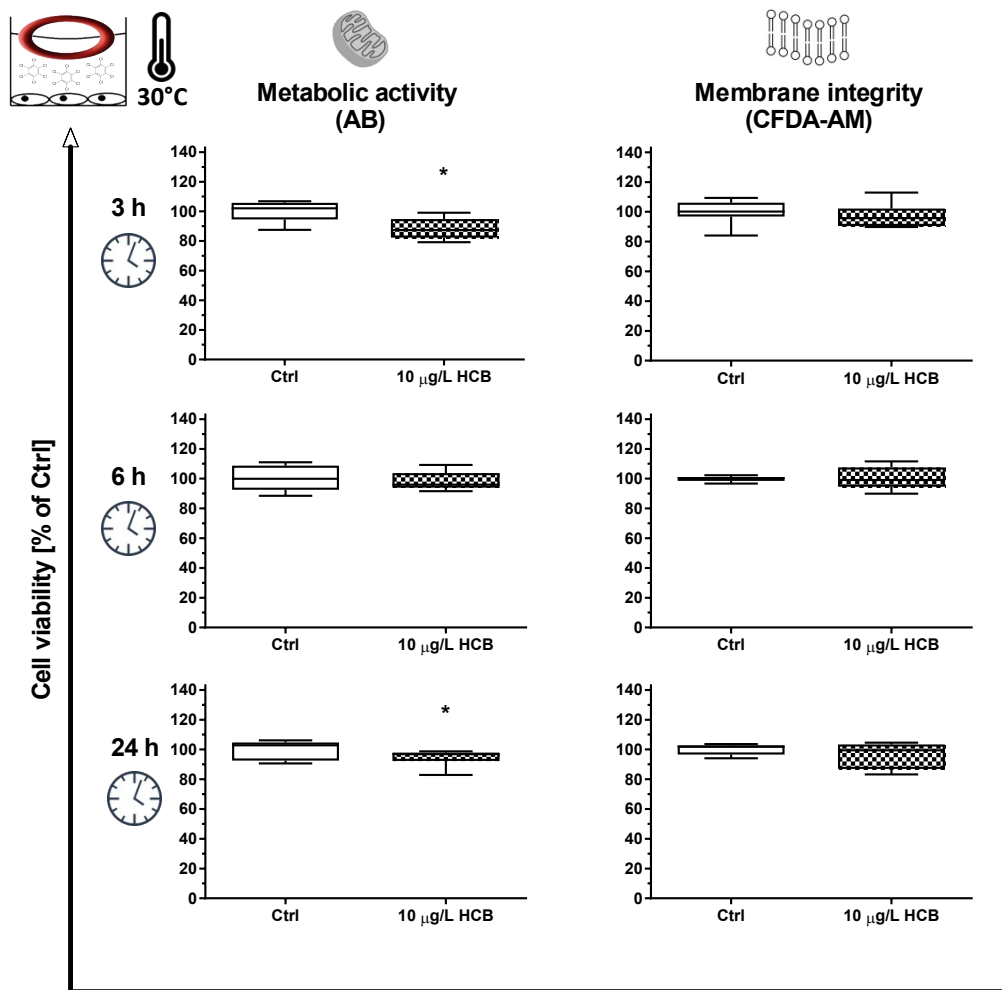
214 **Figure S5. Re-use of O-rings.** Loaded O-rings were extracted after using them up to 5 times in a simulated exposure
215 including 24 hours pre-equilibration of DMEM/F12 medium (1% FBS) and 24 hours exposure in 24-well plates. Each
216 point represents the mean of three technical replicates, error bars represent SD. After each cycle of pre-equilibration
217 and exposure in 24-well plates there is a slight reduction in the concentration of HCB in silicone.

218

219 **2. Effect of HCB on viability of HuWa_{TERT} cells**

220 **2.a. Figure S6**

221

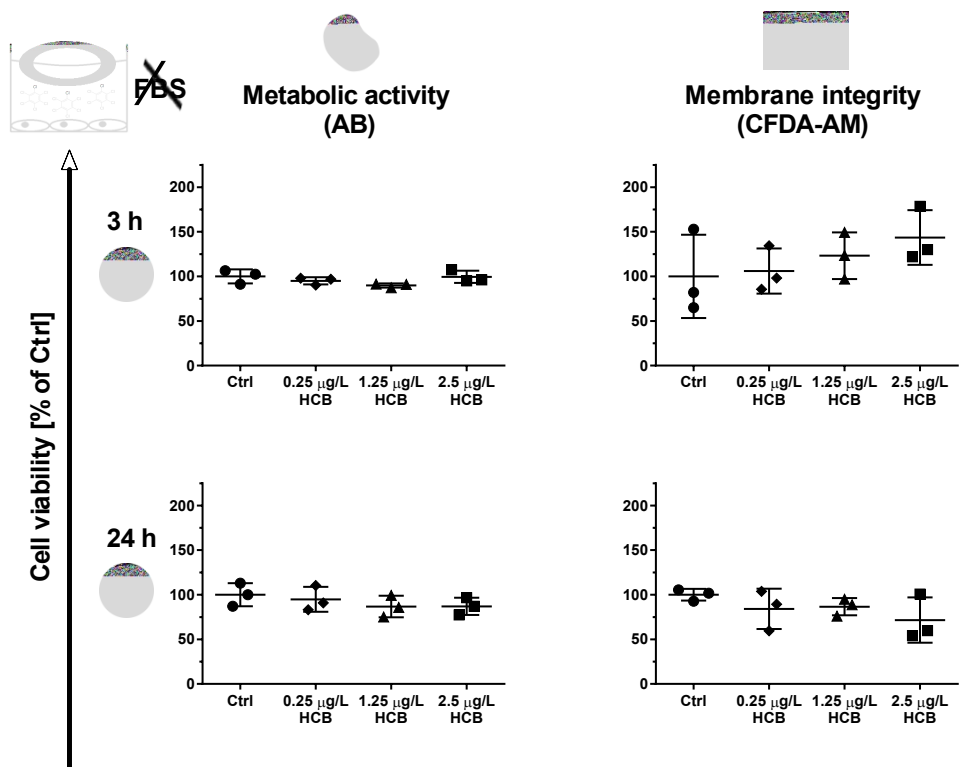


222

223 **Figure S6. Impact of HCB exposure on viability of cells in monolayer under temperature stress.** Attached
 224 monolayers of HuWa_{TERT} were exposed to 10 µg/L HCB using the pre-equilibrated DMEM/F12 (1% FBS) exposure
 225 medium and silicone O-rings for passive dosing at a reduced temperature of 30°C. Metabolic activity and membrane
 226 integrity were assessed relative to control after 3, 6, and 24 hours. Plots represent the median, 1st and 3rd quartile, and
 227 whiskers the 5th and 95th percentile of three biological replicates.

228

229 2.b. Figure S7



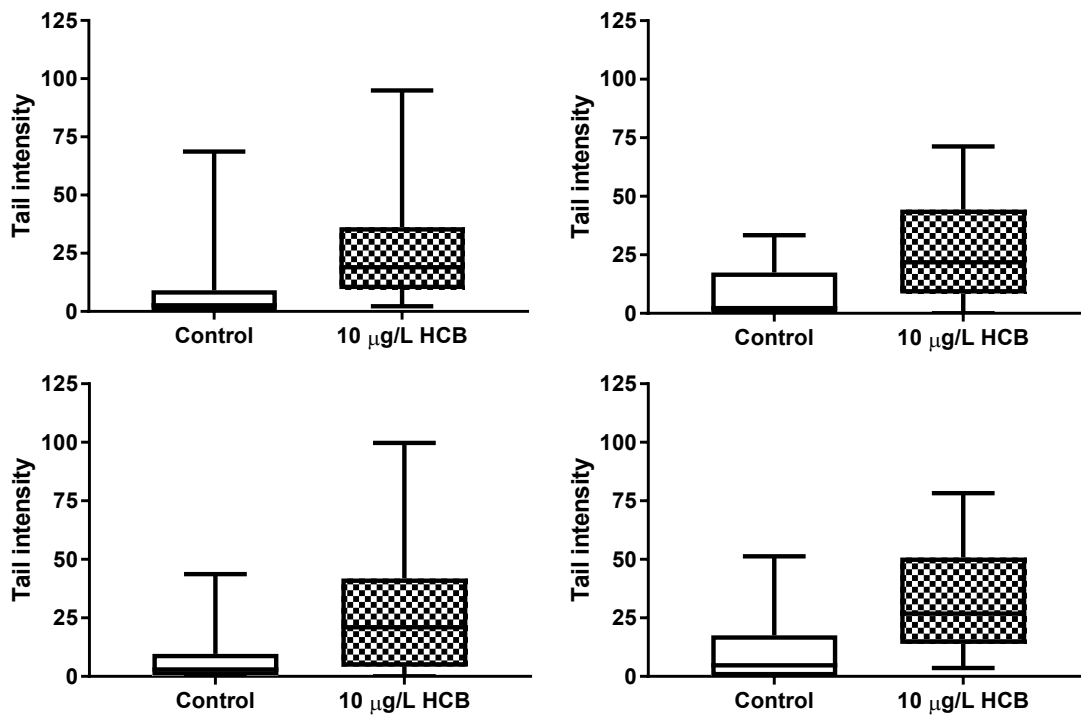
230

231 **Figure S7. Impact of HCB exposure on viability of cells in monolayer with serum-free exposure medium.**
 232 Attached monolayers of HuWa_{TERT} were exposed to 0.25, 1.25, and 2.5 µg/L HCB using the serum-free pre-equilibrated
 233 DMEM/F12 exposure medium and silicone O-rings for passive dosing. Metabolic activity and membrane integrity were
 234 assessed relative to control after 3 and 24 hours. Data represents the mean and error bars the SD of three technical
 235 replicates.

236

237 3. Genotoxic effects of HCB in HuWa_{TERT} cells

238 3.a. Figure S8



239

240 **Figure S8. Visualisation of data obtained in four replicates of the comet assay.** Four biological replicates of the
241 comet assay were performed with HuWa_{TERT} cells after exposure to 10 µg/L HCB for three hours during the phase of
242 attachment to well bottoms using pre-equilibrated DMEM/F12 (1% FBS) exposure medium with passive dosing. Each
243 plot represents the median, 1st and 3rd quartile, and whiskers the 5th and 95th percentile, of one biological replicate with
244 100 analysed cells each in the control and the HCB-treated group.

245

246 **4. References**

- 247 1 N. I. Kramer, F. J. M. Busser, M. T. T. Oosterwijk, K. Schirmer, B. I. Escher and J. L. M.
248 Hermens, Development of a partition-controlled dosing system for cell assays, *Chem. Res.*
249 *Toxicol.*, 2010, **23**, 1806–1814.
- 250 2 G. J. Oostingh, K. E. C. Smith, U. Tischler, I. Radauer-Preiml and P. Mayer, Differential
251 immunomodulatory responses to nine polycyclic aromatic hydrocarbons applied by passive
252 dosing, *Toxicol. Vitro.*, 2015, **29**, 345–351.
- 253 3 K. E. C. Smith, G. J. Oostingh and P. Mayer, Passive Dosing for Defined & Constant
254 Exposure of Hydrophobic Organic Compounds during in Vitro Toxicity Tests, 2010, **23**,
255 55–65.
- 256 4 K. E. C. Smith, N. Dom, R. Blust and P. Mayer, Controlling and maintaining exposure of
257 hydrophobic organic compounds in aquatic toxicity tests by passive dosing, *Aquat. Toxicol.*,
258 2010, **98**, 15–24.
- 259 5 H. Birch, V. Gouliarmou, H. C. H. Lützhof, P. S. Mikkelsen and P. Mayer, Passive dosing
260 to determine the speciation of hydrophobic organic chemicals in aqueous samples, *Anal.*
261 *Chem.*, 2010, **82**, 1142–1146.
- 262 6 J. E. Yordy, R. S. Wells, B. C. Balmer, L. H. Schwacke, T. K. Rowles and J. R. Kucklick,
263 Partitioning of persistent organic pollutants between blubber and blood of wild bottlenose
264 dolphins: Implications for biomonitoring and health, *Environ. Sci. Technol.*, 2010, **44**,
265 4789–4795.
- 266 7 S. M. Bengtson Nash, C. A. Waugh and M. Schlabach, Metabolic concentration of lipid
267 soluble organochlorine burdens in the blubber of southern hemisphere humpback whales
268 through migration and fasting, *Environ. Sci. Technol.*, 2013, **47**, 9404–9413.
- 269 8 R. Cropp, S. M. Bengtson Nash and D. Hawker, A model to resolve organochlorine
270 pharmacokinetics in migrating humpback whales, *Environ. Toxicol. Chem.*, 2014, **33**,
271 1638–1649.
- 272 9 D. Gilbert, P. Mayer, M. Pedersen and A. M. Vinggaard, Endocrine activity of persistent
273 organic pollutants accumulated in human silicone implants - Dosing in vitro assays by
274 partitioning from silicone, *Environ. Int.*, 2015, **84**, 107–114.
- 275 10 P. Mayer, J. Wernsing, J. Tolls, P. G. J. De Maagd and D. T. H. M. Sijm, Establishing and
276 controlling dissolved concentrations of hydrophobic organics by partitioning from a solid
277 phase, *Environ. Sci. Technol.*, 1999, **33**, 2284–2290.
- 278 11 L. M. Jantunen and T. F. Bidleman, Henry's law constants for hexachlorobenzene, p,p'-
279 DDE and components of technical chlordane and estimates of gas exchange for Lake
280 Ontario, *Chemosphere*, 2006, **62**, 1689–1696.

281